REGULAR ARTICLE

blood advances

Multiple mutations at exon 2 of RHOA detected in plasma from patients with peripheral T-cell lymphoma

Barbara Ottolini,[1] Nadia Nawaz,[1,2] Christopher S. Trethewey,[1,2] Sami Mamand,[1,2] Rebecca L. Allchin,[1,2] Richard Dillon,[3] Paul A. Fields,[4] Matthew J. Ahearne,[1,2] and Simon D. Wagner[1,2]

[1]Leicester Cancer Research Centre and [2]Ernest and Helen Scott Haematology Research Institute, University of Leicester, Leicester, United Kingdom; [3]Department of Medical and Molecular Genetics, Faculty of Life Sciences and Medicine, King's College London, London, United Kingdom; and [4]Department of Haematology, Guy's and St. Thomas' Hospital, London, United Kingdom

Key Points

- Multiple RHOA mutations can combine in haplotypes and are detectable in cfDNA from plasma of patients with PTCL.

- Serial cfDNA monitoring of RHOA mutations could allow molecular tracking of disease response in PTCL patients undergoing treatment.

The mutational landscape of peripheral T-cell lymphoma (PTCL) is being revealed through sequencing of lymph node samples, but there has been little work on the mutational load that is present in cell-free DNA (cfDNA) from plasma. We report targeted sequencing of cfDNA from PTCL patients to demonstrate c.50G>T (p.Gly17Val) in RHOA as previously described in angioimmunoblastic T-cell lymphoma (AITL) and a group of PTCL not otherwise specified (NOS) but also detect novel mutations at c.73A>G (p.Phe25Leu) and c.48A>T (p.Cys16*) of exon 2, which were confirmed by Sanger sequencing. In a group of AITL and PTCL-NOS analyzed by droplet digital polymerase chain reaction, 63% (12/19) showed c.50G>T (p.Gly17Val), 53% (10/19) c.73A>G (p.Phe25Leu), and 37% (7/19) c.48A>T (pCys16*). Sequencing of lymph node tissue in 3 out of 9 cases confirmed the presence of c.73A>G (p.Phe25Leu). Inspection of individual sequencing reads from individual patients showed that a single *RHOA* allele could contain >1 mutation, suggesting haplotypes of mutations at *RHOA*. Serial sampling showed changes to *RHOA* mutational frequency with treatment and the apparent occurrence of clones bearing specific haplotypes associated with relapse. Therefore, sequencing of RHOA from cfDNA has revealed new mutations and haplotypes. The clinical significance of these findings will need to be explored in clinical trials, but liquid biopsy might have potential for guiding treatment decisions in PTCL.

Introduction

Peripheral T-cell lymphomas (PTCLs) are rare diseases with a generally poor clinical outlook.[1,2] Gene expression profiling[3,4] has suggested that angioimmunoblastic T-cell lymphoma (AITL), one of the major subtypes of PTCL, is derived from a normal CD4^{+} T-cell subset, T follicular helper (Tfh) cells, and expresses the characteristic surface markers of normal Tfh cells (programmed cell death protein 1 [PD-1] and C-X-C motif chemokine receptor 5 [CXCR5]) and transcription factor (B-cell lymphoma-6 [BCL6]). A proportion (~20%) of another PTCL subtype, PTCL not otherwise specified (NOS), also shows a Tfh-like gene expression pattern and is therefore likely to be related to AITL at the molecular level. The relationship has been strengthened by sequencing studies suggesting a similar mutational landscape with recurrent mutations in the epigenetic modifiers TET2 and DNMT3A[5,6] or in T-cell receptor pathway genes, including CD28[7-9] and PLCG1,[8] or a specific point mutation leading to the substitution of valine for glycine at residue 17 of ras homolog family member A (RHOA c.50G>T [p.Gly17Val]).[10,11] Furthermore, cases with Tfh surface markers tended to show RHOA mutations.[12] Overall there is

The full-text version of this article contains a data supplement.

increasing evidence for the derivation of some T-cell lymphomas from Tfh cells and this has been acknowledged in the most recent update of the World Health Organization classification.[13]

Diagnosis of PTCL can require multiple biopsies, and in addition, interpretation of histopathology and immunocytochemistry can be difficult.[14] Work on lung cancer has suggested that information on genetic aberrations that can be obtained noninvasively might provide valuable support for diagnosis and allow monitoring of response and prediction of relapse.[15,16] RHOA c.50G>T (p.Gly17Val) is detectable by liquid biopsy using cell-free DNA (cfDNA) from plasma[17] of PTCL patients. However, these observations have not been extensively confirmed, and there is little work to investigate how mutational burden in cfDNA varies in response to treatment.

Variant allele frequencies (VAFs) determined from cfDNA generally show good correlations with results from tumor biopsies.[15,18] However, in diffuse large B-cell lymphoma (DLBCL)[19,20] and ovarian cancer,[21] there are indications that some mutations are detectable in plasma, but not tumor. After extensive sequencing of tumor from multiple sites in ovarian cancer, it was shown that the endothelial growth factor receptor mutation, detectable in plasma, was present at a low level at only 1 tissue site. Therefore, analysis of cfDNA can discover mutations not detected in the tumor biopsy, presumably because clones bearing the mutation are anatomically distinct from the biopsy site. Another finding from sequencing of cfDNA in DLBCL is that in some cases VAFs are high (>50%),[18,20] suggesting that tumor DNA makes up a high proportion of cfDNA and indeed total amounts of cfDNA correlate with measures of DLBCL activity such as lactate dehydrogenase and tumor metabolic volume as measured by positron emission tomography-computed tomography (PET-CT) scan.[20,22]

One approach to analyzing cfDNA is to design a targeted sequencing panel using the results of sequencing tumor biopsy specimens as the starting point.[15,18] However, tumor mutational heterogeneity, which is proven in nonhematological cancers,[23,24] suggests multiple tissue biopsies are required to obtain a comprehensive picture of mutational burden. Therefore, although cfDNA integrates the tumor mutational burden from multiple tissue sites,[21,25] mutations that are present in some anatomical sites, but not others, are not likely to be discovered in plasma cfDNA using an experimental approach that relies on biopsy from a single site to derive a targeted panel. Conversely, mutations discovered in the course of sequencing cfDNA might not be detectable at a single tissue biopsy site.

In work reported here, we analyzed mutations in genes previously shown to bear mutations in PTCL primarily using cfDNA from plasma, because cfDNA integrates the mutational burden from different anatomical sites, with a secondary intention to investigate how mutational burden changes during the clinical course. However, we discovered novel RHOA mutations, and we therefore diverted the experimental approach to validate these mutations using an additional sequencing platform, droplet digital polymerase chain reaction (ddPCR) and Sanger sequencing. In addition, we made the observation of RHOA haplotypes (ie, multiple RHOA mutations on a single allele), suggesting a previously unrecognized complexity of RHOA in PTCL.

Materials and methods

Patient samples

Patients enrolled in this study were treated at Leicester Royal Infirmary for newly diagnosed PTCL (n = 23) or relapsed disease (n = 2), including subtypes AITL (n = 10), PTCL-NOS (n = 14), and ALCL (n = 1), as determined by the World Health Organization criteria[13] (supplemental Tables 1 and 2). A total of 43 serial samples were collected from 11 of the patients, while for the remaining 14 patients, only baseline samples were collected (supplemental Table 3). All patient samples were collected with written informed consent for research use and were approved by University Hospitals Leicester R&D (UHL09723) and Health Research Authority National Research Ethics Service Committee East Midlands Research Ethics Committee (REC) number 14/EM/1176. All patients gave written informed consent in accordance with the Declaration of Helsinki. CT or PET-CT scans and laboratory analyses were performed as part of standard clinical care. Diagnosis and PD-1 status was established by 2 expert hematopathologists at University Hospitals Leicester.

Whole-exome sequencing (WES)

Whole-exome capture was performed on DNA isolated from lymph node, peripheral blood mononuclear cells (PBMNCs), and saliva from PTCL_02. DNA was extracted using standard techniques. Libraries were prepared per manufacturer's recommendation using Agilent SureSelect Human All Exon V4 and sequenced at a minimum of 50-bp single-read sequencing on a HiSeq 2000 (Illumina). Mean coverage was 81× with 95.62% of bases covered at ≥20× for the lymph node sample, 117× with 97.65% of bases covered at ≥20× for the PBMNC sample, and 117× with 97.74% of bases covered at ≥20× for the saliva sample.

Targeted next-generation sequencing (NGS)

We designed a cancer personalized profiling by deep sequencing (CAPP-seq) panel with 81 genes and 1029 amplicons covering 299.3 kb.[26] Genes involved in PTCL were incorporated in the panel based on previous literature on the mutational landscape of PTCL and reported in the COSMIC database (https://cancer.sanger.ac.uk/cosmic). Gene Libraries were prepared with the KAPA HTP/LTP Library Prep Kit (Roche, Basel, Switzerland) according to the manufacturer's instructions. After hybridization-based sequence enrichment (Roche), high-throughput sequencing was performed using 2 × 100 or 2 × 150 reads on an Illumina HiSeq 2500 or 4000. Raw sequencing data were mapped to the hg19 reference genome and further processed using a specialized computational workflow that removes PCR duplicates and suppresses technical artifacts. We obtained mean read coverage of 1600× for cfDNA samples. Single-nucleotide variants and indels were genotyped in tumor and plasma samples. Variants with <10 reads (t_alt count) were discarded. Further filtering was carried out such that variants reported by the genome aggregation database (gnomAD) or the Exome Aggregation Consortium (ExAC) were ignored. Variants were also filtered by the Genome Analysis Toolkit (GATK) filtration program, which picks up irregular read bias, germline risk variants, and artifact risk variants.

A second targeted sequencing panel was designed for the Ion-Torrent platform consisting of 66 amplicons across 12 genes (ARID1A, ATM, DNMT3A, FYN, IDH2, JAK2, PLCG1, RHOA,

STAT3, STAT5B, TET2, and TP53). Mutations reported in multiple PTCL cases were prioritized in the panel design phase. For TET2, where no distinct mutational hotspots could be identified, amplicons were designed to maximize the exon's coverage. The Life Tech AmpliSeq Designer tool was used to construct an optimal number of amplicons spanning the mutational hotspots of choice. 10 ng DNA was used as sequencing template for all DNA sources (plasma cfDNA, saliva, and formalin-fixed paraffin-embedded [FFPE] tissue). Sequencing libraries were prepared using the Ion AmpliSeq Library Kit 2.0 (Thermo Fisher Scientific, Waltham, MA) as described previously[27] and run on an Ion PGM sequencer (Thermo Fisher Scientific). DNA libraries from a maximum of 8 samples were pooled on Ion 316v2 sequencing chips. Median sequencing depth across the panel of amplicons was 3200×.

NGS data were filtered and analyzed using the quality control metrics described previously.[28] Variants were identified using Ion Torrent variant calling software (v4.2.1.0). To derive limits of detection DNA from normal subjects (PBMNCs and matched cfDNA n = 6, FFPE tonsil n = 2), patients with solid organ cancers (PBMNCs and matched cfDNA n = 4) and matched patient saliva samples (n = 5) were sequenced. For Ion Torrent variant, detection thresholds were 1% VAF for both cfDNA and FFPE samples, and similarly for CAPP-seq, these were determined to be 1% VAF for cfDNA.

All variants were manually examined using the Integrative Genomics Viewer (IGV) software, curated, and approved before being accepted into the analysis.

To infer phylogenetic trees from the IGV read pileup data and calculated longitudinal RHOA haplotype frequencies, the following principles were used[29]: (1) a subclone carries the same mutation as the founding clone and mutations are not lost during evolution, (2) multiple mutations on a single read occur in the same clone, (3) hierarchy of phased mutations can be determined by relative proportions, and (4) significant differential changes in mutation VAFs suggest separate phylogenetic branch (the "crossing rule").

Sample collection and plasma cfDNA extraction

Blood was collected into EDTA tubes, and plasma and PBMNCs were separated by centrifugation. Samples were collected from a single center, and transit times before processing were ~1 hour. Following separation by centrifugation, plasma and buffy coat were stored at −80°C until extraction.

Plasma cfDNA was then isolated using the QIAamp Circulation Nucleic Acid kit (Qiagen, Hilden, Germany) according to the manufacturer's instructions. Concentrations were then determined using the Qubit dsDNA HS assay kit (Thermo Fisher Scientific) for plasma and the Qubit dsDNA BR assay kit (Thermo Fisher Scientific) for PBMNCs according to the manufacturer's instructions. Genomic DNA from FFPE lymph node cores was extracted using the ReliaPrep FFPE gDNA Miniprep kit (Promega, Madison, WI) according to the manufacturer's instructions. DNA concentration and purity were measured using a Qubit fluorometer (Thermo Fisher Scientific).

ddPCR

ddPCR was used as independent validation technology to confirm the RHOA mutational status and the VAFs of all patient samples analyzed by NGS, whenever enough DNA was available for confirmation. Three different in-house TaqMan assays were designed (supplemental Table 4) to target in the first channel one of the 3 RHOA mutations c.73A>G (p.Phe25Leu), c.48A>T (p.Cys16*), and c.50G>T (p.Gly17Val) and in the second channel the corresponding RHOA wild-type allele to provide an accurate VAF calculation. Between 5 and 10 ng DNA was used for each reaction on a Bio-Rad QX200 ddPCR system as previously described.[30]

cfDNA was amplified using ddPCR supermix for probes (Bio-Rad, Hercules, CA). DNA (10 ng at 1 ng/μL) was added to ddPCR supermix for probes (11 μL) (Bio-Rad) and primer/probe mix (1.1 μL). The reaction mix was transferred to a DG8 cartridge with droplet generation oil (75 μL) for probes (Bio-Rad). Droplets were then transferred to a 96-well plate and sealed, after which the plate was transferred to a thermal cycler and droplets were analyzed in the QX200 Droplet Reader and gating applied based on control samples. Using Quantasoft analysis software, data were analyzed to obtain the fractional abundance (FA) of the mutated alleles. FA is calculated as follows: FA (%) = (N_{mut} /(N_{mut} + N_{wt}) × 100), where N_{mut} is the number of mutant events and N_{wt} is the number of wild-type events in each reaction. ddPCR controls (no template, salmon sperm DNA, and normal subject DNA) were always included, and any samples with <10 000 total droplets were repeated.

Numbers of false-positive droplets from 8 patients with non-hematological cancers were analyzed by Poisson distribution (supplemental Table 5) to derive limits of detection. The following number of droplets was accepted as a true positive: >4 droplets in the channel detecting the c.73A>G (p.Phe25Leu) mutation, >2 droplets for the c.48A>T (p.Cys16*) mutation, and >1 droplet for the c.50G>T (p.Gly17Val) mutation.

Results

WES of a single case reveals a novel RHOA mutation, c.73A>G (p.Phe25Leu)

Initial studies to compare the mutational burden represented by liquid and tissue biopsy in PTCL involved WES of synchronous PBMNCs and lymph node tissue from a single patient with AITL (PTCL_02) (supplemental Table 6). Mutations in genes previously implicated in PTCL (TET2, IDH2, and VAV1) and a novel mutation in IL12RB1 exon10, c.A1068T (p.Arg356Ser), a cytokine receptor relevant for T-cell function, were detected in lymph node. PBMNCs did not show mutations of TET2, IDH2, and VAV1, but a RHOA change (c.73A>G) predicted to lead to p.Phe25Leu was detected. This mutation has not previously been reported, but p.Phe25Val has recently been described in lung cancer.[31] Phenylalanine at residue 25 is part of an α helix that appears to interact with phenylalanine at position 171, and the bulky aliphatic side chains of both valine and leucine would be predicted to disrupt this interaction (supplemental Figure 1).

This case demonstrated presumptive evidence for peripheral blood lymphoma cells. However, work from others[32] suggested circulating tumor DNA was present in 98% of DLBCL patients,[22] whereas a separate study showed circulating lymphoma cells were detectable in only ~50% of PTCL patients. Therefore, we chose to use cfDNA rather than PBMNCs in this study, because only a fraction of patients will have detectable circulating lymphoma cells, but cfDNA is likely to be present in almost all and has been shown to

reflect global tissue mutational heterogeneity[15,33] in hematological malignancy.

Targeted and Sanger sequencing and ddPCR from cfDNA

cfDNA was obtained in amounts comparable to that of other series of patients with lymphoma,[18,34] but there was no significant association with lactate dehydrogenase, clinical stage, or international prognostic index (supplemental Figure 2). Using an Illumina CAPP-seq protocol (n = 5) the previously characterized c.50G>T (p.Gly17Val) missense mutation was detected together with novel mutations c.73A>G (p.Phe25Leu) and c.48A>T (p.Cys16*) (Figure 1A; supplemental Table 7). All 5 RHOA exons were included in the sequencing, and no significant mutations outside exon 2 were found (supplemental Figure 3). Mutations in epigenetic modifiers and T-cell receptor signaling proteins (Figure 1A) were also detected in line with previous work.

To provide orthogonal validation for novel RHOA mutations, 3 individual ddPCRs (supplemental Figure 4) were established (n = 19). Overall, ≥1 RHOA mutation was detected in 12 out of 19 patients (63%): c.73A>G (p.Phe25Leu) in 10 out of 19 patients (53%), c.50G>T (p.Gly17Val) in 12 out of 19 patients (63%), and c.48A>T (p.Cys16*) in 7 out of 19 patients (37%) (Figure 1B). To extend our findings, a more focused targeted sequencing panel of 12 genes, including TET2 (supplemental Table 8), was designed for an Ion Torrent platform (n = 16) (supplemental Figure 5). As expected, multiple mutations were detected in TET2 (14 separate mutations across 6 of the 16 patients sequenced). Significant correlations were detected between RHOA mutant allele frequencies detected by ddPCR and Ion Torrent sequencing, including c.50G>T (p.Gly17Val) (R^2 = 0.65, $P < .0001$), c.73A>G (p.Phe25Leu) (R^2 = 0.974, $P < .0001$), and c.48A>T (p.Cys16*) (R^2 = 0.862, $P < .0001$) (Figure 1C; supplemental Table 9). In those cases analyzed by both CAPP-seq and Ion Torrent, the correlation between RHOA VAFs detected by the 2 platforms was $R^2 = 0.91$ ($P < .0001$) (supplemental Figure 6), and all mutations detected by one technology were also detected by the other. Sanger sequencing provided further evidence for the 3 RHOA mutations (Figure 1D). DNA from normal subjects (PBMNCs and matched cfDNA n = 6, tonsil n = 2) and patients with solid organ cancers (PBMNCs and matched cfDNA n = 4) were sequenced, and no RHOA mutations were detected. To exclude constitutive changes, DNA extracted from saliva was sequenced in 5 out of 16 patients (supplemental Table 1) without detection of RHOA mutations.

Targeted sequencing of tissue biopsy samples

Previous work on patients with malignant disease has noted that mutations can be present in cfDNA while not being detectable in tissue, although there is support for the idea that such mutations might be present either at low frequency or in specific anatomical sites in tissues.[19,21] Accordingly we carried out Ion Torrent sequencing of single cores from 11 patients of which 9 patients had sufficient coverage for assessment (supplemental Table 10); 3 out of 9 patients showed c.73A>G (p.Phe25Leu) with VAFs of 4.5% (PTCL_02), 2.7% (PTCL_21), and 6.6% (PTCL_23). Comparing frequencies of all the mutations detected (ie, in RHOA, TET2, IDH2, DNMT3A, and TP53) confirmed that RHOA mutations were readily detectable in cfDNA rather than tissue, whereas

mutations in the other genes were detectable from both sources of DNA (Figure 2A). We considered the possibility that RHOA mutations were not homogenously distributed in a lymph node section by carrying out multiple biopsies on 3 samples with sufficient lymph node material (supplemental Table 10). Of these, 1 case (Figure 2B) showed RHOA mutations in 1 out of 4 cores, while TET2 mutations were present in all 4 cores. This case demonstrated heterogeneity of RHOA mutations within a single lymph node biopsy.

Multiple RHOA mutations can exist on the same allele

RHOA mutations occurred, on a single Ion Torrent amplicon, within a short stretch of exon 2 around the guanosine triphosphate binding site. For the whole group of patients, c.73A>G (p.Phe25Leu) was present as a single mutation on 27.7% ± 8% (mean ± standard error of the mean) of reads, c.50G>T (p.Gly17Val) on 6.4% ± 7% of reads, and c.48A>T (p.C16*) on 0.3% ± 0.1% of reads (supplemental Figure 7). However, c.73A>G (p.Phe25Leu) and c.50G>T (p.Gly17Val) occurred on the same allele in 2% ± 0.7% of reads, while c.73A>G (p.Phe25Leu) and c.48A>T (p.C16*) occurred on 12.5% ± 4% of reads. Read pileups (Figures 3) and, in some cases Sanger sequencing (supplemental Figure 8) confirmed mutations occurring together on the same allele. The pileups also suggest some mutual exclusivity in that c.50G>T (p.Gly17Val) and c.48A>T (p.C16*) do not occur together (see PTCL_10 and PTCL_22, Figure 3). These observations suggest mutational complexity at the RHOA locus, which is in line with data from adult T-cell leukemia (ATLL)[35] but has not previously been reported by sequencing of DNA from lymph nodes in PTCL.

Changes to RHOA haplotypes and mutational burden during the course of disease

Serial plasma samples were taken during the course of treatment (n = 5), and VAFs of individual RHOA mutations were determined (Figure 4A-E). Disappearance of detectable RHOA mutations associated with radiological remission in 2 cases (Figure 4A-B). In a further patient (Figure 4C), RHOA mutations remained detectable once a radiological remission had been obtained but an increase in c.50G>T (p.Gly17Val) anticipated clinical relapse at a new anatomical site, while in the fourth patient, partial remission was associated with reduction in RHOA VAFs and relapse with c.50G>T (p.Gly17Val), but we observed that as disease progressed further, there was loss of mutant RHOA (Figure 4D). The last patient (Figure 4E) showed clinical progression after CHOP and was treated with IVE to achieve a partial response. Further chemotherapy with GDP produced a complete response, which was consolidated by autologous stem cell transplantation.

Next, we analyzed haplotype changes over time in patient PTCL_25 (Figure 5) to infer clonal architecture.[29] Of the reads showing a mutation at the initial time point (T1) (Figure 5A), 65.5% show a single founder RHOA variant, c.73A>G (p.Phe25Leu), and 25% bear this mutation together with c.48A>T (p.C16*). We therefore infer a dominant clone bearing a single mutation with a subclone bearing 2 mutations. At timepoint 4 (T4) (Figure 5B) c.50G>T (p.Gly17Val) is a single founder mutation accounting for 26.4% of the mutated reads, while 11% bear this mutation combined with c.73A>G (p.Phe25Leu). Therefore, we infer that at T4, the dominant clone shows a single c.50G>T (p.Gly17Val) mutation with a subclone bearing 2 mutations. It is noteworthy that the
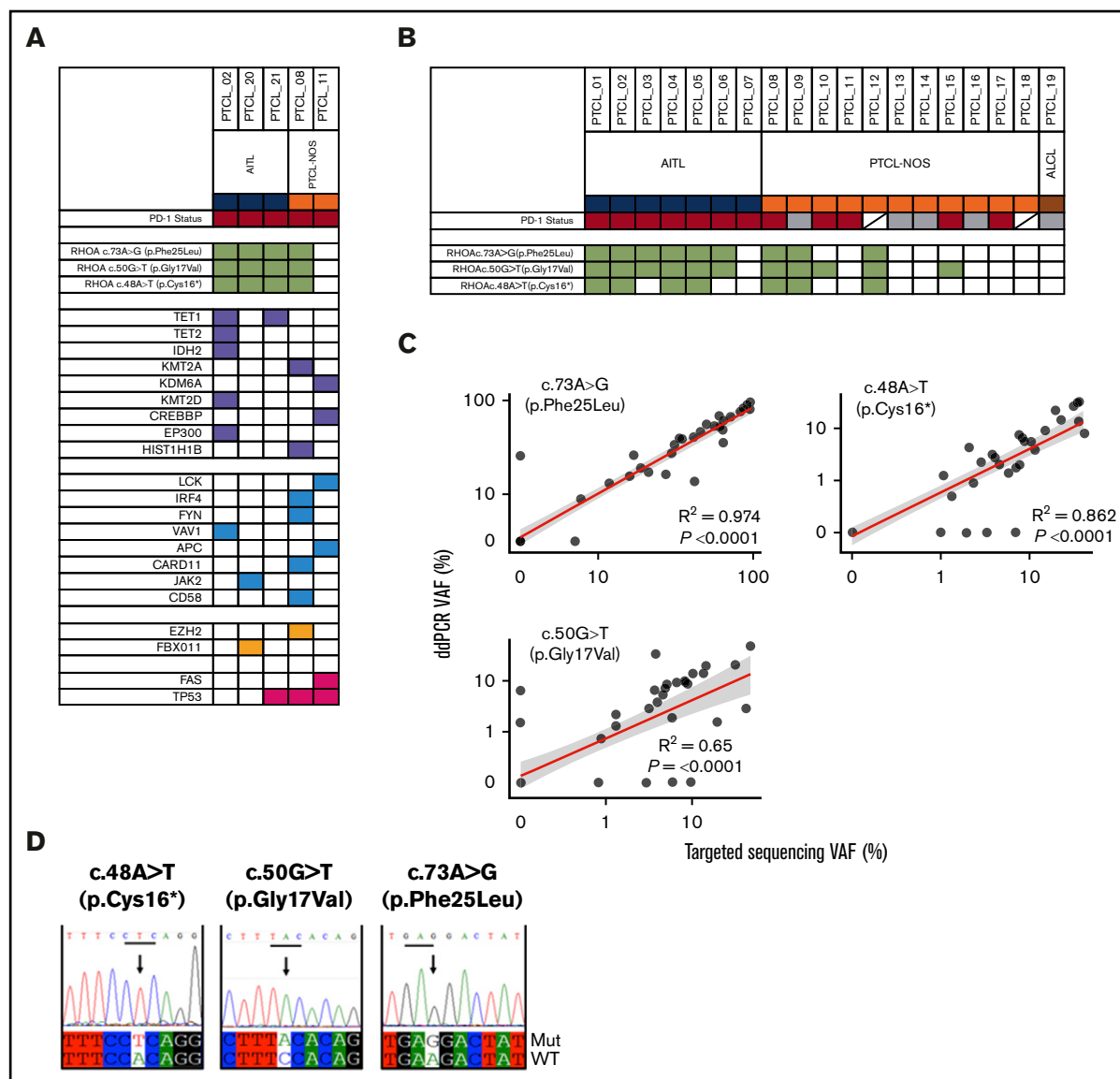
Figure 1. RHOA mutations detected in peripheral blood. (A) The results of targeted deep sequencing from cfDNA of RHOA exon 2 by Illumina CAPP-seq. Mutations were detected at presentation (n = 5) at c.50G>T (p.Gly17Val), c.73A>G (p.Phe25Leu), and c.48A>T (pCys16*). Diagnosis (either AITL or PTCL-NOS) is indicated. In all cases, the malignant T-cells expressed PD-1. (B) ddPCR assays from cfDNA for the 3 RHOA mutations. Diagnosis and PD-1 status are shown. Red shading indicates PD-1 expression; for cases with gray shading, PD-1 is negative, and for those with a diagonal line, PD-1 is not determined. (C) Mutational frequency by ddPCR results was correlated with VAF from Ion Torrent sequencing for the 3 RHOA mutations in samples at presentation and during the course of treatment (28 samples from 21 patients). Linear regression (red line) and 95% confidence interval are shown. For c.50G>T (p.Gly17Val), $R^2 = 0.65$ and $P = .0001$; for c.73A>G (p.Phe25Leu), $R^2 = 0.974$ and $P = .0001$; and for c.48A>T (pCys16*), $R^2 = 0.862$ and $P = .0001$. (D) Sanger sequencing fluorograms from cloned PCR product showing the 3 RHOA mutations c.50G>T, c.73A>G, and c.48A>T (pCys16*). Mut, mutated; WT, wild-type.

inferred subclone, c.50G>T (p.Gly17Val) with c.73A>G (p.Phe25-Leu), is present at a low level at timepoints T2 and T3 (Figure 4C).

Overall, we can infer clonal architecture at the RHOA locus as shown in the tree diagram (Figure 5C). Single mutations, either c.50G>T (p.Gly17Val) or c.73A>G (p.Phe25Leu), appear to arise independently, following which subclones evolve such that, in this case, c.50G>T (p.Gly17Val) is associated with c.73A>G (p.Phe25Leu) at timepoint T1 and c.73A>G (p.Phe25Leu) is associated with c.48A>T (p.C16*) at T4.

Next, we investigated changes to individual RHOA mutations and haplotypes (Figure 5D-E). At early time points, the greatest number of reads showed c.73A>G (p.Phe25Leu) alone, with smaller numbers demonstrating 2 mutations, c.73A>G (p.Phe25Leu) with c.48A>T (p.C16*). In both cases analyzed here, c.50G>T (p.Gly17Val)–bearing reads were present at very low level at T1 but subsequently (T4) expanded. At T4, the dominant mutation was c.50G>T (p.Gly17Val) alone, with smaller numbers of reads showing both c.50G>T (p.Gly17Val) and c.73A>G (p.Phe25Leu).
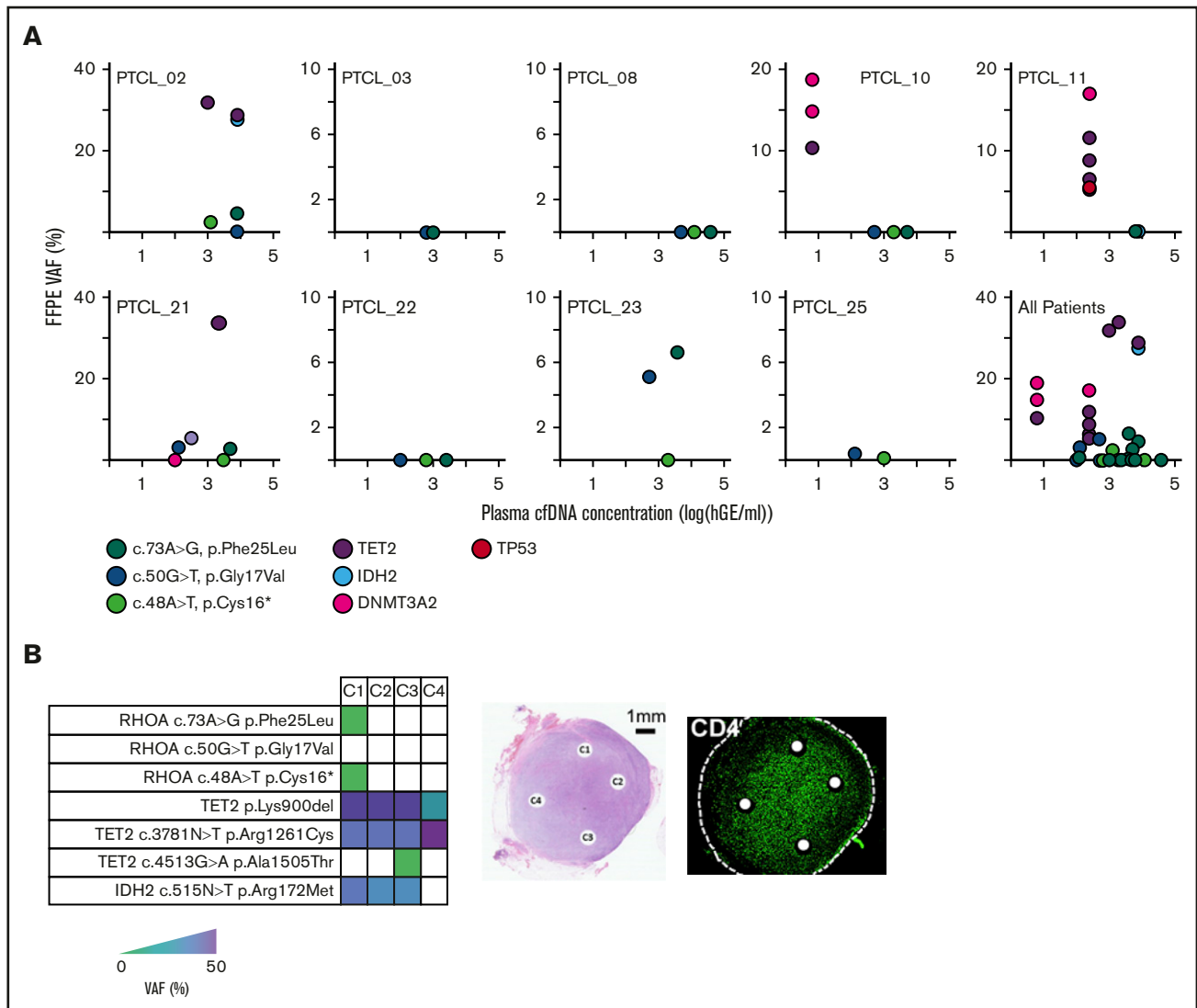
Figure 2. Comparison of targeted sequencing using DNA from plasma or FFPE lymph node sections. (A) Plots compare amounts of mutation in plasma (human genome equivalents [hGE]) with VAF (%) in lymph node from FFPE tissue. Results are presented for 9 individual cases together with a combined plot of all patients. Individual RHOA mutations and other detected and mutated genes are color coded as shown. (B) Four cores were sequenced from a single lymph node. Results of the sequencing are indicated in the table with a color scale being used to indicate the VAF. Middle panel shows a hematoxylin and eosin–stained lymph node section indicating the positions of cores labeled C1 to C4. Right panel shows immunofluorescence staining of a sequential lymph node section to show heterogeneity of CD4 staining.

Here, we showed that RHOA VAFs, detectable from cfDNA at lymphoma presentation, are reduced on treatment, markedly with complete clinical remission (Figure 4A-B,E), and less so with partial clinical remission (compare T1 and T2 of Figure 4C-D), increasing again at relapse (compare T2 to T3 of Figure 4C-D). Secondly, we suggest that there are changes to RHOA haplotypes during the course of disease (Figure 5).

Discussion

Our main findings are that RHOA mutations not readily detectable from lymph node biopsies are present in cfDNA from plasma, and secondly, that these mutations can combine on a single allele to form haplotypes that can be tracked during the course of disease. Specifically we found novel mutations c.73A>G (p.Phe25Leu) and

c.48A>T (p.Cys16*) in exon 2 of RHOA that have not previously been described in sequencing lymph node tissue.

There have been studies showing good concordance between tissue and plasma mutation detection in DLBCL,[18] Waldenström macroglobulinemia,[36] and myeloma[37] as well as in nonhematological malignancy.[38,39] However, the literature has precedents, as mentioned above,[19,21] for discordance between cfDNA and tissue mutation detection. A further study reported that small deletions causing reversion mutations of BRCA2 were detectable in cfDNA, but not tissue in prostate cancer patients.[40] The most likely cause of this apparent paradox is tumor heterogeneity; ie, malignant cells with varying patterns of mutation are present in anatomically separate areas of tumor.[15,23,24,41] Mutations detected in cfDNA integrate the entire mutational burden of a tumor; therefore, variants
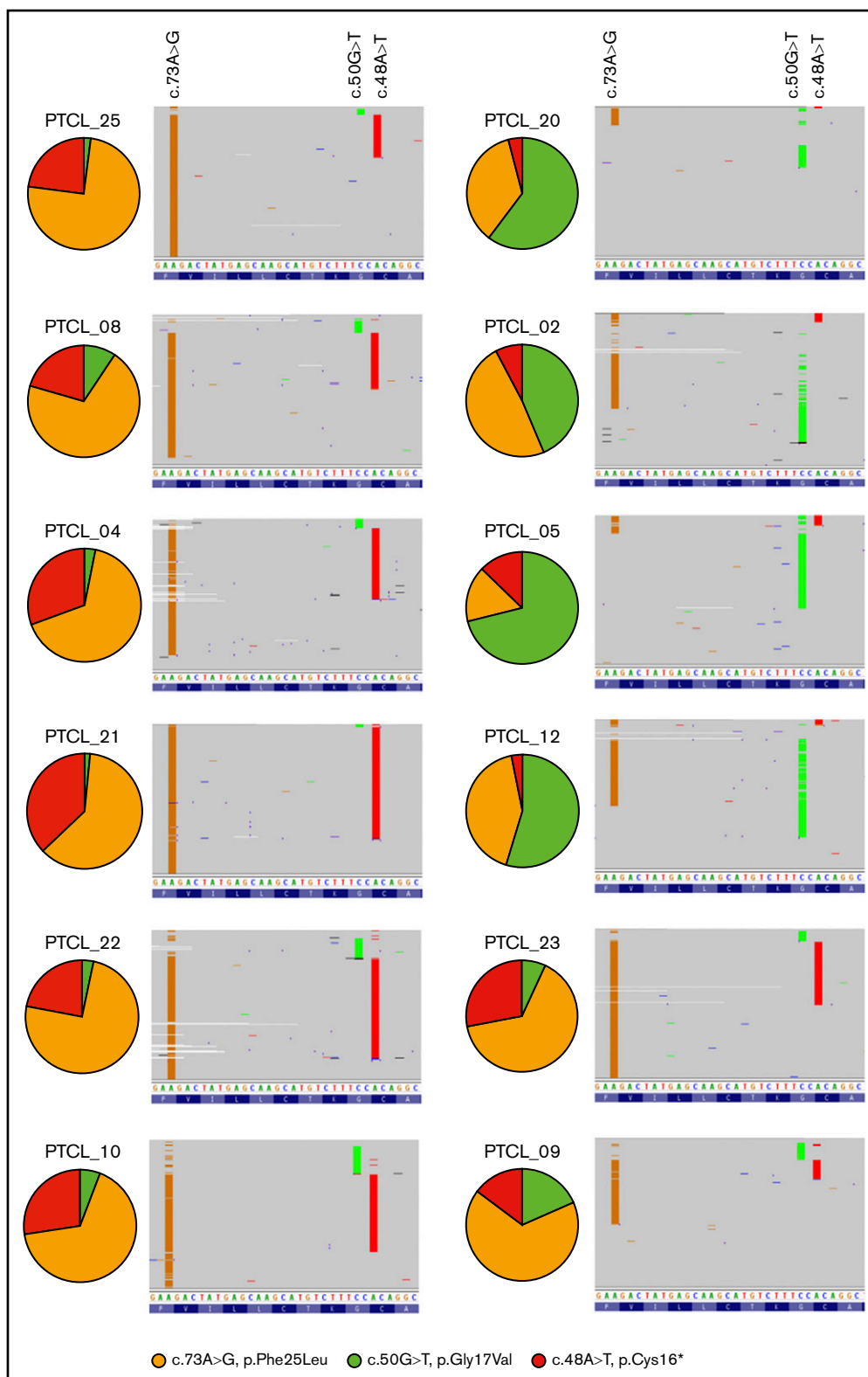
Figure 3. RHOA mutational frequencies and haplotypes vary between individuals. Haplotypes at RHOA exon 2 from each PTCL case in which the baseline plasma sample contained a total RHOA mutational burden (VAF) >10%. The pie chart represents the proportions of each individual exon 2 mutation as a fraction of all reads bearing a RHOA mutation. Panels to the right show down-sampled read pileups (representing ~10% of all reads) with the position of mutations indicated above and the DNA sequence below.
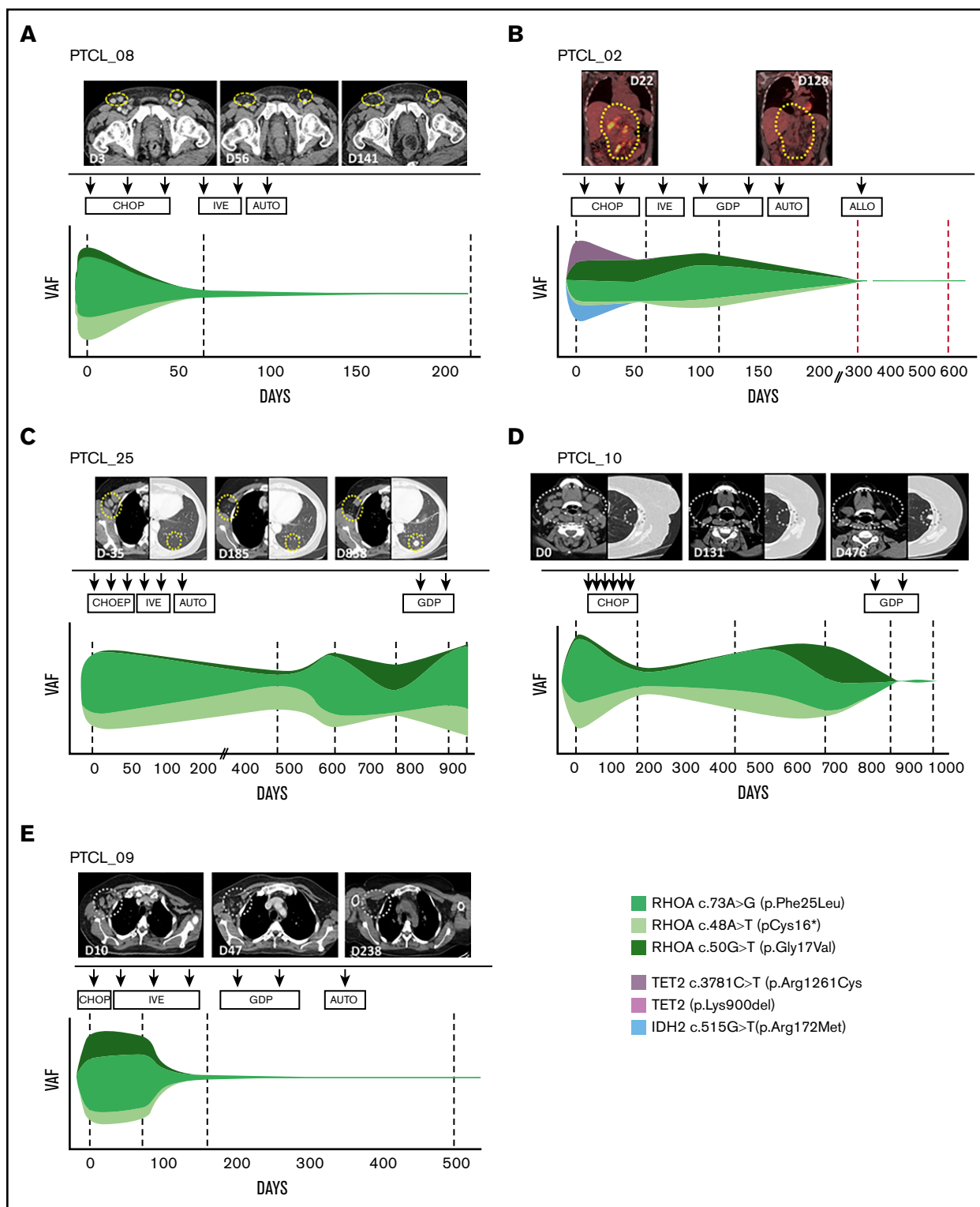
Figure 4. RHOA mutations can be followed over time and correlate with radiological measures of response. Clonal tides representing mutation dynamics for RHOA and, where possible, TET2 and IDH2, during treatment of 5 PTCL cases. VAFs are plotted as indicated by the color key to the lower right. The dotted vertical lines indicate the points at which samples were taken. (A) PTCL_08 was treated with cyclophosphamide, Adriamycin, vincristine, and prednisolone (CHOP) chemotherapy and achieved a radiological complete response. Subsequent consolidation was with ifosfamide, epirubicin, and etoposide (IVE) followed by a lomustine, etoposide, cytarabine, melphalan (HDT/LEAM)–conditioned autologous stem cell transplant. Data were obtained from Ion Torrent sequencing. (B) PTCL_02 had disease refractory to 2 lines of chemotherapy (CHOP and IVE) before achieving a PET-negative response with gemcitabine, dexamethasone, and cisplatin (GDP). Treatment was then consolidated with an autologous followed by an allogeneic stem cell transplant. The data for the 4 timepoints indicated by black dotted lines are taken from Ion Torrent sequencing data and those
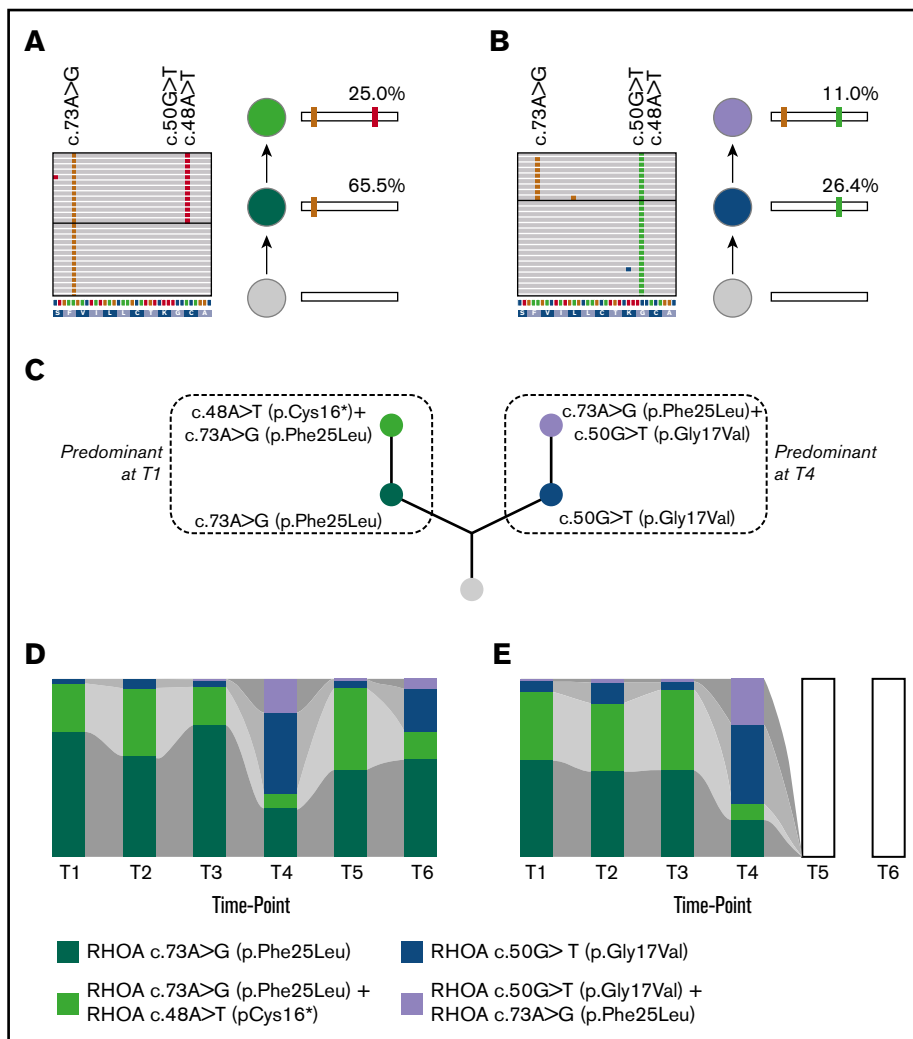
Figure 5. Inferred clonal architecture of RHOA mutations and changes to RHOA mutations or haplotypes over time. IGV pileups from a single patient, PTCL_25, (Figure 4C) at 2 timepoints T1 (A) and T4 (B). The data are interpreted to show evolution from a wild-type gene sequence to one showing 2 mutations via a gene sequence bearing a single mutation as shown in the panels to the right of the read pileups. (C) Inferred phylogenetic tree inferred from IGV read pileups. At T1 the dominant clone bears a single c.73A>G (p.Phe25Leu) (dark green) with a subclone that shows both c.73A>G (p.Phe25Leu) and c.48A>T (pCys16*) (light green). At the later timepoint, T4, the dominant clone bears a single c.50G>T (p.Gly17Val) (blue) with a subclone bearing c.50G>T (p.Gly17Val) and c.73A>G (p.Phe25Leu) (purple). Analysis showed the same RHOA phylogenetic tree for both PTCL_10 and PTCL_25. The branch of the tree to the left shows the inferred predominant clonal arrangement at the early timepoint (T1) whereas the branch to the right shows the clones, which emerge at timepoint, T4. For both cases stacked bar charts show the relative frequencies of RHOA mutations or haplotypes in PTCL_25 (D) and PTCL_10 (E). The empty columns indicate that samples were analyzed at these timepoints but that no mutant RHOA was detected. The phylogenetic tree derived from the haplotype data for PTCL_10 is identical to that of PTCL_25 (Figure 5C).

that are detectable from this source of DNA might not be present in DNA from a single tissue biopsy. This is clearly a difficult hypothesis to prove, but sequencing of multiple tissue sites has revealed mutations not present in the primary biopsy site in some reported cases.[15,21] In those patients in which RHOA mutations were detected in cfDNA, we were able to also detect the mutation in lymph node DNA. In one case in which we sequenced multiple cores from a single lymph node sample, we found that although TET2 mutations were present in all 4 cores, RHOA mutations were only present in one of these. We therefore suggest that analysis of cfDNA in PTCL integrates an unexpected mutational heterogeneity at the RHOA locus. Recent work has demonstrated that multiple T-cell receptor β rearrangements are detectable in 15% of patients

with AITL, and this evidence also suggests previously unexpected clonal complexity in PTCL.[42]

However, a line of work on lung cancer has suggested another possibility that might contribute to both high levels of specific mutation in plasma cfDNA, but not tissue, and high circulating VAFs. In a comparison of tissue and plasma VAFs, the authors produced an index quantitating the efficiency with which DNA from specific subclones was shed from tissue into the plasma.[43] They showed that specific driver mutations were preferentially shed into the plasma. There is little work on this phenomenon in other diseases, but clearly, if such a mechanism occurred in PTCL, it would provide an explanation for our results.

Figure 4. (continued) indicated by red dotted lines from ddPCR. (C) PTCL_25 was treated with CHOP with etoposide (CHOEP) chemotherapy but did not respond and then received IVE followed by HDT/LEAM autologous stem cell transplant. PTCL recurred 2 years later, and reinduction chemotherapy with GDP achieved a transient partial response before further progression occurred and the patient died. Data were obtained from Ion Torrent sequencing. (D) PTCL_10 was treated with CHOP chemotherapy and achieved a partial remission on CT scan. The remission lasted ~18 months, but she then represented with a rising peripheral blood lymphocyte count, pruritus, and skin lesions. CT scan (day 476) showed lung nodules. Lymph node biopsy confirmed relapsed lymphoma, and she was retreated with GDP. In this case, loss of mutant RHOA after GDP was associated with disease progression. Data were obtained from Ion Torrent sequencing. (E) PTCL_09 was treated with CHOP chemotherapy but progressed clinically and was treated with IVE, achieving a partial response. The response was consolidated with GDP and autologous stem cell transplantation. Data were obtained from ddPCR.

RHOA mutations are a feature of ATLL,[35] but in distinction to Tfh lymphoma in which a single c.50G>T (p.Gly17Val) mutation predominates, there are multiple mutations in individual cases and sometimes on individual alleles with potentially opposing functional consequences. The role of RHOA in ATLL is likely to be complex and is currently unclear.[44] Our report, in line with the ATLL study, suggests that RHOA mutation is also complex in PTCL. Animal models demonstrate that c.50G>T (p.Gly17Val), in combination with TET2 mutation, contributes to Tfh cell proliferation and lymphomagenesis.[45-47] Our observations (Figure 5D-E) suggest dynamic changes to RHOA mutation, as detected in plasma, during the course of disease, but the functional and clinical consequences require further studies.

Clonal hematopoiesis[48] is a confounding factor in liquid biopsy studies.[49] RHOA is not known to be involved in clonal hematopoiesis; therefore, we believe there is a very low likelihood that this contributed to our results. TET2 and DNMT3A are genes implicated in clonal hematopoiesis, but there is a large amount of evidence showing that they are mutated in PTCL.[5,6,10,11] The novel RHOA mutations, c.73A>G (p.Phe25Leu) and c.48A>T (p.Cys16*), were not only found by targeted sequencing (in some cases by both CAPP-seq and Ion Torrent platforms) but also validated by ddPCR and confirmed by Sanger sequencing. Further evidence suggesting that the mutations are derived from lymphoma is that they disappeared from the peripheral blood in cases responding to treatment (Figure 4).

We suggest that further investigation of cfDNA in larger studies of PTCL will give insights into tumor heterogeneity, and potentially, longitudinal studies will demonstrate how changes to RHOA mutation or haplotype frequency associate with disease progression or response to treatment.

Authorship

Contribution: B.O., N.N., S.M., R.L.A., and C.S.T. designed and performed research; P.A.F. and R.D. performed research, analyzed data, and critically reviewed the paper; and M.J.A. and S.D.W. designed research, analyzed data, and wrote the paper.

Conflict-of-interest disclosure: The authors declare no competing financial interests.

The current affiliation for S.M. is Polytechnic Research Center, Erbil Polytechnic University, Kurdistan Regional Government, Erbil, Kurdistan.

ORCID profiles: C.S.T., 0000-0001-9128-3533; S.M., 0000-0001-7014-5481; R.D., 0000-0001-9333-5296; P.A.F., 0000-0001-5288-8898; S.D.W., 0000-0002-8914-0370.

Correspondence: Simon D. Wagner, University of Leicester, Room 104, Hodgkin Building, Lancaster Rd, Leicester LE1 7HB, United Kingdom; e-mail: sw227@le.ac.uk; or Matthew J. Ahearne, University of Leicester, Room 104, Hodgkin Building, Lancaster Rd, Leicester LE1 7HB, United Kingdom; e-mail: mja40@le.ac.uk.

References

1. Foss FM, Zinzani PL, Vose JM, Gascoyne RD, Rosen ST, Tobinai K. Peripheral T-cell lymphoma. *Blood*. 2011;117(25):6756-6767.

2. Vose J, Armitage J, Weisenburger D; International T-Cell Lymphoma Project. International peripheral T-cell and natural killer/T-cell lymphoma study: pathology findings and clinical outcomes. *J Clin Oncol*. 2008;26(25):4124-4130.

3. de Leval L, Rickman DS, Thielen C, et al. The gene expression profile of nodal peripheral T-cell lymphoma demonstrates a molecular link between angioimmunoblastic T-cell lymphoma (AITL) and follicular helper T (TFH) cells. *Blood*. 2007;109(11):4952-4963.

4. Piccaluga PP, Agostinelli C, Califano A, et al. Gene expression analysis of peripheral T cell lymphoma, unspecified, reveals distinct profiles and new potential therapeutic targets. *J Clin Invest*. 2007;117(3):823-834.

5. Couronné L, Bastard C, Bernard OA. TET2 and DNMT3A mutations in human T-cell lymphoma. *N Engl J Med*. 2012;366(1):95-96.

6. Lemonnier F, Couronné L, Parrens M, et al. Recurrent TET2 mutations in peripheral T-cell lymphomas correlate with TFH-like features and adverse clinical parameters. *Blood*. 2012;120(7):1466-1469.

7. Vallois D, Dobay MPD, Morin RD, et al. Activating mutations in genes related to TCR signaling in angioimmunoblastic and other follicular helper T-cell-derived lymphomas. *Blood*. 2016;128(11):1490-1502.

8. Manso R, Rodríguez-Pinilla SM, González-Rincón J, et al. Recurrent presence of the PLCG1 S345F mutation in nodal peripheral T-cell lymphomas. *Haematologica*. 2015;100(1):e25-e27.

9. Rohr J, Guo S, Huo J, et al. Recurrent activating mutations of CD28 in peripheral T-cell lymphomas. *Leukemia*. 2016;30(5):1062-1070.

10. Palomero T, Couronné L, Khiabanian H, et al. Recurrent mutations in epigenetic regulators, RHOA and FYN kinase in peripheral T cell lymphomas. *Nat Genet*. 2014;46(2):166-170.

11. Sakata-Yanagimoto M, Enami T, Yoshida K, et al. Somatic RHOA mutation in angioimmunoblastic T cell lymphoma. *Nat Genet*. 2014;46(2):171-175.

12. Watatani Y, Sato Y, Miyoshi H, et al. Molecular heterogeneity in peripheral T-cell lymphoma, not otherwise specified revealed by comprehensive genetic profiling. *Leukemia*. 2019;33(12):2867-2883.

13. Swerdlow SH, Campo E, Pileri SA, et al. The 2016 revision of the World Health Organization classification of lymphoid neoplasms. *Blood*. 2016;127(20): 2375-2390.

14. Herrera AF, Crosby-Thompson A, Friedberg JW, et al. Comparison of referring and final pathology for patients with T-cell lymphoma in the National Comprehensive Cancer Network. *Cancer*. 2014;120(13):1993-1999.

15. Abbosh C, Birkbak NJ, Wilson GA, et al; PEACE consortium. Phylogenetic ctDNA analysis depicts early-stage lung cancer evolution [published correction appears in *Nature*. 2018;554(7691):264]. *Nature*. 2017;545(7655):446-451.

16. Nong J, Gong Y, Guan Y, et al. Circulating tumor DNA analysis depicts subclonal architecture and genomic evolution of small cell lung cancer [published correction appears in *Nat Commun*. 2019;10(1):552]. *Nat Commun*. 2018;9(1):3114.

17. Sakata-Yanagimoto M, Nakamoto-Matsubara R, Komori D, et al. Detection of the circulating tumor DNAs in angioimmunoblastic T- cell lymphoma. *Ann Hematol*. 2017;96(9):1471-1475.

18. Scherer F, Kurtz DM, Newman AM, et al. Distinct biological subtypes and patterns of genome evolution in lymphoma revealed by circulating tumor DNA. *Sci Transl Med*. 2016;8(364):364ra155-364ra155.

19. Rossi D, Diop F, Spaccarotella E, et al. Diffuse large B-cell lymphoma genotyping on the liquid biopsy. *Blood*. 2017;129(14):1947-1957.

20. Bohers E, Viailly PJ, Becker S, et al. Non-invasive monitoring of diffuse large B-cell lymphoma by cell-free DNA high-throughput targeted sequencing: analysis of a prospective cohort. *Blood Cancer J*. 2018;8(8):74.

21. Murtaza M, Dawson S-J, Tsui DWY, et al. Non-invasive analysis of acquired resistance to cancer therapy by sequencing of plasma DNA. *Nature*. 2013; 497(7447):108-112.

22. Kurtz DM, Scherer F, Jin MC, et al. Circulating tumor DNA measurements as early outcome predictors in diffuse large B-cell lymphoma. *J Clin Oncol*. 2018;36(28):2845-2853.

23. Gerlinger M, Rowan AJ, Horswell S, et al. Intratumor heterogeneity and branched evolution revealed by multiregion sequencing. *N Engl J Med*. 2012; 366(10):883-892.

24. Burrell RA, McGranahan N, Bartek J, Swanton C. The causes and consequences of genetic heterogeneity in cancer evolution. *Nature*. 2013;501(7467): 338-345.

25. Dawson S-J, Tsui DWY, Murtaza M, et al. Analysis of circulating tumor DNA to monitor metastatic breast cancer. *N Engl J Med*. 2013;368(13): 1199-1209.

26. Mamanova L, Coffey AJ, Scott CE, et al. Target-enrichment strategies for next-generation sequencing. *Nat Methods*. 2010;7(2):111-118.

27. Page K, Guttery DS, Fernandez-Garcia D, et al. Next generation sequencing of circulating cell-free DNA for evaluating mutations and gene amplification in metastatic breast cancer. *Clin Chem*. 2017;63(2):532-541.

28. Jovelet C, Ileana E, Le Deley M-C, et al. Circulating cell-free tumor DNA analysis of 50 genes by next-generation sequencing in the prospective MOSCATO trial. *Clin Cancer Res*. 2016;22(12):2960-2968.

29. Nik-Zainal S, Alexandrov LB, Wedge DC, et al; Breast Cancer Working Group of the International Cancer Genome Consortium. Mutational processes molding the genomes of 21 breast cancers. *Cell*. 2012;149(5):979-993.

30. Hindson BJ, Ness KD, Masquelier DA, et al. High-throughput droplet digital PCR system for absolute quantitation of DNA copy number. *Anal Chem*. 2011;83(22):8604-8610.

31. Zehir A, Benayed R, Shah RH, et al. Mutational landscape of metastatic cancer revealed from prospective clinical sequencing of 10,000 patients [published correction appears in *Nat Med*. 2017;23(8):1004]. *Nat Med*. 2017;23(6):703-713.

32. Delfau-Larue M-H, de Leval L, Joly B, et al. Targeting intratumoral B cells with rituximab in addition to CHOP in angioimmunoblastic T-cell lymphoma. A clinicobiological study of the GELA. *Haematologica*. 2012;97(10):1594-1602.

33. Parikh AR, Leshchiner I, Elagina L, et al. Liquid versus tissue biopsy for detecting acquired resistance and tumor heterogeneity in gastrointestinal cancers [published correction appears in *Nat Med*. 2019;25(12):1949]. *Nat Med*. 2019;25(9):1415-1421.

34. Delfau-Larue M-H, van der Gucht A, Dupuis J, et al. Total metabolic tumor volume, circulating tumor cells, cell-free DNA: distinct prognostic value in follicular lymphoma. *Blood Adv*. 2018;2(7):807-816.

35. Nagata Y, Kontani K, Enami T, et al. Variegated RHOA mutations in adult T-cell leukemia/lymphoma. *Blood*. 2016;127(5):596-604.

36. Bagratuni T, Ntanasis-Stathopoulos I, Gavriatopoulou M, et al. Detection of MYD88 and CXCR4 mutations in cell-free DNA of patients with IgM monoclonal gammopathies. *Leukemia*. 2018;32(12):2617-2625.

37. Manier S, Park J, Capelletti M, et al. Whole-exome sequencing of cell-free DNA and circulating tumor cells in multiple myeloma. *Nat Commun*. 2018;9(1): 1691.

38. Leighl NB, Page RD, Raymond VM, et al. Clinical utility of comprehensive cell-free DNA analysis to identify genomic biomarkers in patients with newly diagnosed metastatic non-small cell lung cancer. *Clin Cancer Res*. 2019;25(15):4691-4700.

39. García-Foncillas J, Tabernero J, Élez E, et al. Prospective multicenter real-world RAS mutation comparison between OncoBEAM-based liquid biopsy and tissue analysis in metastatic colorectal cancer. *Br J Cancer*. 2018;119(12):1464-1470.

40. Quigley D, Alumkal JJ, Wyatt AW, et al. Analysis of circulating cell-free DNA identifies multiclonal heterogeneity of *BRCA2* reversion mutations associated with resistance to PARP inhibitors. *Cancer Discov*. 2017;7(9):999-1005.

41. Alizadeh AA, Aranda V, Bardelli A, et al. Toward understanding and exploiting tumor heterogeneity. *Nat Med*. 2015;21(8):846-853.

42. Yao WQ, Wu F, Zhang W, et al. Angioimmunoblastic T-cell lymphoma contains multiple clonal T-cell populations derived from a common TET2 mutant progenitor cell. *J Pathol*. 2020;250(3):346-357.

43. Mao X, Zhang Z, Zheng X, et al. Capture-based targeted ultradeep sequencing in paired tissue and plasma samples demonstrates differential subclonal ctDNA-releasing capability in advanced lung cancer. *J Thorac Oncol*. 2017;12(4):663-672.

44. Ishikawa S. Opposite RHOA functions within the ATLL category. *Blood*. 2016;127(5):524-525.

45. Cortés JR, Ambesi-Impiombato A, Couronné L, et al. RHOA G17V Induces T Follicular Helper Cell Specification and Promotes Lymphomagenesis. *Cancer Cell*. 2018;33(2):259-273.e7.

46. Ng SY, Brown L, Stevenson K, et al. RhoA G17V is sufficient to induce autoimmunity and promotes T-cell lymphomagenesis in mice. *Blood*. 2018; 132(9):935-947.

47. Zang S, Li J, Yang H, et al. Mutations in 5-methylcytosine oxidase TET2 and RhoA cooperatively disrupt T cell homeostasis. *J Clin Invest*. 2017;127(8): 2998-3012.

48. Genovese G, Kähler AK, Handsaker RE, et al. Clonal hematopoiesis and blood-cancer risk inferred from blood DNA sequence. *N Engl J Med*. 2014; 371(26):2477-2487.

49. Hu Y, Ulrich BC, Supplee J, et al. False positive plasma genotyping due to clonal hematopoiesis. *Clin Cancer Res*. 2018;24(18):4437-4443.